life

MDPI

Article

Development and Validation of Multiplex Real-Time PCR Assays for Allele Discrimination and Genotyping of *ABCG2* Q126X and Q141K

Kang-Hee Lee [1,†], Min Young Park [1,†], Hye Soo Jung [1], Dohsik Minn [2], Yong-Hak Sohn [1] and Yong-Jin Yang [1,*]

[1] Department of Molecular Diagnostics, Seegene Medical Foundation, Seoul 02637, Republic of Korea; l23058@mf.seegene.com (K.-H.L.); pyli186@mf.seegene.com (M.Y.P.); hsjung@mf.seegene.com (H.S.J.); medsohn@mf.seegene.com (Y.-H.S.)
[2] Automated Laboratory Center, Seegene Medical Foundation, Seoul 02637, Republic of Korea; dsmin@mf.seegene.com
* Correspondence: yjyang@mf.seegene.com
† These authors contributed equally to this work.

Abstract

Gout is a metabolic disorder caused by chronic hyperuricemia, which leads to monosodium urate crystal deposition and subsequent inflammatory arthritis. Genetic factors, particularly those regulating urate transport, play a major role in susceptibility to hyperuricemia and gout. Among these, the functional *ABCG2* variants Q126X (rs72552713) and Q141K (rs2231142) are well-established genetic determinants of impaired urate excretion. In this study, we developed a hydrolysis probe-based multiplex real-time polymerase chain reaction (PCR) assay for allele discrimination and genotyping of the *ABCG2* Q126X and Q141K variants in separate reactions. This assay demonstrated high analytical specificity without cross-reactivity in both synthetic and clinical samples and maintained reliable genotype detection across clinically relevant DNA concentrations. In method comparison using 1653 clinical samples, the multiplex real-time PCR assay showed complete concordance with Sanger sequencing (Cohen's $\kappa = 1.00$). Combined genotype analysis (Q126X/Q141K) demonstrated a gene dose-dependent association with serum uric acid levels and hyperuricemia risk, consistent with the estimated ABCG2 transport function. These findings indicate that the developed assay provides a reliable and practical molecular tool for rapid *ABCG2* genotyping and genetic risk assessment of hyperuricemia and gout.

Keywords: *ABCG2*; hyperuricemia; gout; multiplex real-time PCR (mRT-PCR)

Check for updates

Academic Editor: Da-Tian Bau

Received: 28 August 2026
Revised: 21 October 2026
Accepted: 21 October 2026
Published: 26 October 2026

Copyright: © 2026 by the authors. Licensee MDPI, Basel, Switzerland. This article is an open access article distributed under the terms and conditions of the Creative Commons Attribution (CC BY) license.

1. Introduction

Gout, an inflammatory arthritis, arises from hyperuricemia and the deposition of monosodium urate crystals in joints [1,2]. This metabolic disorder affects millions of people worldwide, causing gout flares and imposing a substantial socioeconomic burden if not adequately treated [1,3]. Hyperuricemia develops when uric acid production from purine catabolism exceeds its elimination [4]. Increased production can result from increased purine intake or enhanced endogenous purine turnover, whereas reduced elimination can result from impaired renal or intestinal excretion [5]. These processes are influenced by both environmental and genetic factors. Lifestyle factors, including dietary habits, can influence urate levels, while genetic variation is a major determinant of inter-individual differences in serum uric acid (SUA) concentrations [6–9]. Genome-wide association studies have

consistently identified variants in urate transport genes as major determinants of gout risk, with these variants playing a central role in defining SUA levels and susceptibility to gout [8,10–15].

ATP-binding cassette subfamily G member 2 (*ABCG2*) is among the most strongly associated genes with SUA levels and gout susceptibility [10–12,16–23]. *ABCG2* encodes a high-capacity urate exporter expressed in the kidney, liver, and intestines; its dysfunction markedly reduces urate clearance [24–26]. Two loss-of-function variants of *ABCG2*, Q126X (c.376C > T, rs72552713) and Q141K (c.421C > A, rs2231142), have been extensively studied as major genetic risk factors for gout [17,27–31]. In East Asian populations, Q141K is the most prevalent and well-characterized gout risk allele (minor allele frequency [MAF] = 0.3034), whereas Q126X is rare (MAF = 0.0084) based on allele frequency data from the Allele Frequency Aggregator (ALFA) Release 5, version 20260205170148. Despite its low frequency, Q126X exerts a strong functional effect on urate transport [16–18,31]. The combined genotypes of these *ABCG2* variants (Q126X/Q141K) are significantly associated with elevated SUA levels and increased risk of hyperuricemia and gout [19,32].

Because Q126X and Q141K impair ABCG2 function to different extents, combined genotype analysis provides a biologically interpretable framework for estimating the overall degree of ABCG2-mediated urate transport dysfunction. Q126X is a nonsense variant that produces a non-functional allele, whereas Q141K is generally treated as a partially functional allele with approximately half of the urate transport activity of the wild-type allele [19]. On this basis, previous studies have classified Q126X/Q141K genotype combinations into estimated ABCG2 transport function categories, including full function, 3/4 function, 1/2 function, and ≤1/4 function, rather than evaluating each single nucleotide polymorphism (SNP) independently [19,32–35]. This classification has shown a graded relationship with gout susceptibility and related urate phenotypes, supporting the clinical relevance of combined genotyping of both variants for genetic risk assessment of hyperuricemia and gout [17,19,32].

Multiple studies have conducted *ABCG2* SNP genotyping using hydrolysis probe-based real-time polymerase chain reaction (PCR) and SYBR Green methods [33,34,36–38]. However, detailed PCR conditions, analytical performance characteristics, and clinical validation of the assay have not been evaluated [36,37]. Therefore, a standardized real-time PCR assay with clearly characterized analytical performance is needed for accurate and reliable genotyping of *ABCG2* variants. Since Q126X and Q141K are predefined functional variants with established biological relevance, a targeted assay is more cost-effective and suitable for routine laboratory implementation than broader sequencing-based approaches. Standardization of assay design and reaction conditions is expected to improve reproducibility and facilitate inter-laboratory implementation of *ABCG2* genotyping.

The objective of this study was to develop and validate a multiplex real-time PCR assay for allele discrimination and genotyping of the *ABCG2* Q126X and Q141K variants. We designed and evaluated the assay to provide a practical tool for the early assessment of individuals at an increased risk of hyperuricemia and gout.

2. Materials and Methods

2.1. Blood Samples and Serum Uric Acid Measurement

The Institutional Review Board of the Seegene Medical Foundation approved the study (SMF-IRB-2024-020). We analyzed residual ethylenediaminetetraacetic acid-anticoagulated whole blood (EDTA W/B) samples from 1653 individuals for whom SUA levels were measured using a Labospect 008 α automatic analyzer (Hitachi, Tokyo, Japan) as part of routine health examinations or clinical testing in September 2024. For categorical analysis, hyperuricemia was defined using general sex-specific reference cut-offs of >7.0 mg/dL in males

and >5.7 mg/dL in females, consistent with those used in NHANES-based studies [1,39] and a separate clinical cohort study [40].

2.2. Genomic DNA Extraction

Genomic DNA was extracted from EDTA-W/B samples during collection using the MagNA PURE 96 system (Roche, Basel, Switzerland) following the manufacturer's instructions. A 200 µL aliquot of whole blood was loaded into the processing cartridge, and DNA was eluted in 100 µL of elution buffer. The concentration and purity of the isolated DNA were assessed using a NanoDrop One spectrophotometer (Thermo Fisher Scientific, Waltham, MA, USA). All DNA samples were stored at −80 °C until further analysis.

2.3. Primer/Probe Design

The assay consisted of two separate reaction tubes: one for Q126X and the other for Q141K. Each reaction simultaneously detected the wild-type allele, variant allele, and internal control using multiplex real-time PCR. DNA oligonucleotides were designed based on the reference sequence of the *ABCG2* gene (accession number: NG_032067.2; https://www.ncbi.nlm.nih.gov/gene, accessed on 1 July 2024). For each SNP, one primer pair flanking each variant site and two minor groove binding (MGB) hydrolysis probes were designed [41]. A FAM (6-fluorescein amidite) labeled probe was designed to hybridize with the wild-type allele (c.376C for Q126X and c.421C for Q141K), while a VIC-labeled probe targeted the respective mutant allele (c.376T and c.421A). The probes were designed such that they differed at the SNP level to distinguish single-nucleotide mismatches. The *HBB* gene was used as an internal control (IC). Primers were designed using dual-priming oligonucleotide (DPO) technology to increase specificity, as previously reported [42]. All DNA oligonucleotide sequences are listed in Table 1. GeneRunner version 6.0 was used to calculate the melting temperatures of the DNA oligonucleotides.

Table 1. Oligonucleotide primers and probes for genotyping Q126X and Q141K variants.

Target Gene	Type	Sequence (5′-3′)	Position *	Concentration (µM)	Tm (°C)
ABCG2 Q126X	F primer	5′-AGATCCAAGTGGATTATCTGGAG AIIIIITGATAAATGG-3′	104,433 to 104,471	0.5	58.5
	R primer	5′-AAGCTGCTGTAAAGAAC GTCAGTIIIIIGACCATGTCA-3′	104,614 to 104,651	0.5	57.8
	Wild-type probe (c.376C)	5′-FAM-ACGTGGTA**C**AAGTA-MGBNFQ-3′	104,510 to 104,523	0.15	25.7
	Mutant probe (c.376T)	5′-VIC-ACGTGGTA**T**AAGTA-MGBNFQ-3′	104,510 to 104,523	0.25	22.8
ABCG2 Q141K	F primer	5′-TCATTAAAATGCTATTTGCCTTA AGIIIIITGTTGTGATG-3′	105,085 to 105,124	0.5	58.4
	R primer	5′-CTGCCACTTTATCCA GACCTAACTIIIIIATGACCCTGT-3′	105,216 to 105,254	0.5	58.9
	Wild-type probe (c.421C)	5′-FAM-CTGAGAACT**G**TAAGT-MGBNFQ-3′	105,147 to 105,161	0.75	22.4
	Mutant probe (c.421A)	5′-VIC-CTGAGAACT**T**TAAGT-MGBNFQ-3′	105,147 to 105,161	0.25	23.9

Table 1. *Cont.*

Target Gene	Type	Sequence (5′-3′)	Position *	Concentration (μM)	Tm (°C)
HBB (internal control)	F primer	5′-GGCATAAAAGTCAGGGCAGAIIIIICTATTGCT-3′	4967 to 4999	0.25	56.9
	R primer	5′-CCAACTTCATCCACGTTCACCIIIIICCACAGGG-3′	5091 to 5124	0.25	59.0
	probe †	5′-Cy5- CCTGAGGAGAAGTCTGCCGTTACTGC -BHQ2-3′	5066 to 5091	0.25	68.8
	probe †	5′-Cy5.5- CCTGAGGAGAAGTCTGCCGTTACTGC -BHQ2-3′	5066 to 5091	0.1	68.8

Bold and underlined indicate the c.376C > T (wild type: C, mutant: T) or c.421C > A (wild type: C, mutant: A) target nucleotides. * Position of primer, probe indicates range of oligonucleotide binding sequences according to reference sequences (https://www.ncbi.nlm.nih.gov/gene, accession number *ABCG2* NG_032067.2 and HBB NG_059281.1, accessed on 1 July 2024). The amplicon sizes of *ABCG2* Q126X, *ABCG2* Q141K, and *HBB* are 219 bp, 170 bp, and 158 bp, respectively. † The internal control probe was labeled with Cy5 for Q141K tube and Cy5.5 for the Q126X tube. F primer, forward primer; I, internal deoxyinosine modification; R primer, reverse primer; Tm, melting temperature.

2.4. Multiplex Real-Time PCR Conditions

SNP genotyping of *ABCG2* Q126X and Q141K was performed using two separate multiplex real-time PCR reactions, one for each variant, on the CFX96 instrument (Bio-Rad Laboratories, Irvine, CA, USA). Each reaction was performed in a separate tube with a total volume of 20 μL, comprising 10 μL of 2× PCR enzyme (Enzynomics, Daejeon, Republic of Korea), 5 μL of extracted genomic DNA (30–90 ng/μL), and 5 μL of oligonucleotide mixture (final concentrations are described in Table 1). PCR conditions were as follows: initial denaturation at 95 °C for 15 min, followed by 40 cycles of denaturation at 95 °C for 10 s, and annealing/extension at 62 °C for 30 s. To prevent false-negative results, *HBB* was included as an endogenous IC as previously described.

For genotype calling, the fluorescence threshold was set at 1500 RFU for all four channels (FAM, VIC, Cy5, and Cy5.5). Allele detection was determined by amplification signals crossing the corresponding threshold. In reactions with detectable *HBB* IC amplification, detection in the FAM channel alone indicated a homozygous wild-type genotype (Q126X C/C or Q141K C/C), detection in both FAM and VIC indicated a heterozygous genotype (Q126X C/T or Q141K C/A), and detection in the VIC channel alone indicated a homozygous variant genotype (Q126X T/T or Q141K A/A). The *HBB* IC signal was assessed in the Cy5.5 channel for the Q126X reaction and the Cy5 channel for the Q141K reaction. Reactions without detectable *HBB* IC amplification were classified as invalid regardless of the allele-specific signals. Reactions with detectable IC amplification but no interpretable allele-specific pattern were classified as no calls.

2.5. Sanger Sequencing of ABCG2 Variants for Genotype Confirmation

Sanger sequencing was performed to confirm the Q126X and Q141K genotypes of *ABCG2*. A 977-bp region encompassing *ABCG2* exons 4 and 5 was amplified using a single primer pair (forward: 5′-AGCATGTGTTGGAGGGAAAA-3′; reverse: 5′-TGCTGATCATGATGCTTTCAG-3′), each at 0.5 μM. PCR was performed with an initial denaturation at 94 °C for 15 min, followed by 35 cycles of 94 °C for 30 s, 61 °C for 40 s, and 72 °C for 1 min, with a final extension at 72 °C for 5 min. Bidirectional Sanger sequencing was performed using both primers. Sanger sequencing was performed using the BigDye Terminator v3.1 cycle sequencing kit (Thermo Fisher Scientific, Waltham, MA, USA) and a 3500 Genetic Analyzer (Thermo Fisher Scientific). Sequencing chromatograms were examined using the FinchTV v1.4.0 software (Geospiza Inc., Seattle, WA, USA) and Variant Reporter software (version 3.0; Thermo Fisher Scientific).

Chromatograms were reviewed at the target variant positions to assess peak clarity and identify single or overlapping peaks corresponding to homozygous or heterozygous genotypes, respectively. Genotype assignments were confirmed by agreement between forward and reverse sequencing results.

2.6. Analytical Specificity

Four synthetic DNAs (Cosmo Genetech, Seoul, Republic of Korea): *ABCG2* exon 4 with c.376C, exon 4 with c.376T, exon 5 with c.421C, and exon 5 with c.421A were used to evaluate analytical specificity. These sequences were synthesized at positions 104,380–104,726 (347 bp) for exon 4 and 104,966–105,312 (347 bp) for exon 5 in the reference sequence (NG_032067.2). A synthesized DNA fragment concentration of 1 pg/reaction was used to evaluate specificity in triplicate.

2.7. Analytical Sensitivity Assessment

Analytical sensitivity was assessed using serially diluted clinical DNA samples representing each target allele (c.376C, c.376T, c.421C, and c.421A). Each allele was evaluated separately using a corresponding clinical specimen to assess allele detection across the tested DNA concentrations. Three samples were used for each variant type, except for the T/T genotype for Q126X variant, for which only one sample was available because of its low frequency. Each nucleic acid was serially diluted from an undiluted concentration: extracted nucleic acid stock (50–80 ng/μL) to 1×10^{1}, 1×10^{0}, 1×10^{-1}, 1×10^{-2}, and 1×10^{-3} ng/μL. The assay was performed in triplicate to ensure reproducibility. Ct values at each concentration were summarized as mean ± standard deviation (SD).

To further assess analytical sensitivity, four synthetic plasmid DNA materials representing the four target alleles (c.376C, c.376T, c.421C, and c.421A) were individually serially diluted from 1×10^{1} pg/reaction to 1×10^{-3} pg/reaction and tested in triplicate at each concentration.

2.8. Precision of the Multiplex Real-Time PCR Assays

Intra-assay repeatability and inter-assay reproducibility were evaluated using 47 clinical DNA samples. For Q126X, the sample set comprised 28 C/C, 18 C/T, and one T/T sample; for Q141K, it comprised 20 C/C, 18 C/A, and nine A/A samples. The same specimens were tested for both variants. Intra-assay repeatability was assessed by duplicate measurements of each sample within the same run and plate, whereas inter-assay reproducibility was assessed across three independent runs on the same CFX96 instrument. Mean Ct values were calculated across replicate measurements. The SD was calculated as the pooled within-sample SD across repeated measurements, and the coefficient of variation (CV) was calculated as SD/mean Ct × 100.

2.9. Analysis of SUA Levels by ABCG2 Genotype

The association between *ABCG2* genotype and SUA levels was evaluated for the Q126X and Q141K variants, and MAFs were determined. For each variant, individuals were classified into wild-type, heterozygous and homozygous mutant genotype groups. The analyses were stratified by sex (male, female, and total population). Detailed MAFs, genotype distribution, and SUA levels according to individual *ABCG2* genotypes are provided in Supplementary Table S1.

2.10. Hyperuricemia Risk by Combined ABCG2 Genotype

The risk of hyperuricemia was evaluated based on the combined *ABCG2* genotype (Q126X/Q141K). Individuals were classified based on their *ABCG2* Q126X and Q141K genotypes and grouped into four functional categories (full, 3/4, 1/2, and ≤1/4 function)

according to estimated ABCG2 transport activity [19,32–34]. Odds ratios (ORs) and 95% confidence intervals (CIs) were calculated using the wild-type genotype combination (C/C for Q126X and C/C for Q141K) as the reference group.

2.11. Statistical Analysis

Data were analyzed using R software version 4.4.2. SUA levels in the three genotype groups (C/C, C/A, and A/A) were assessed using one-way analysis of variance (ANOVA), followed by Tukey's honestly significant difference (HSD) post hoc test, for the Q141K variant. For the Q126X variant, due to the low frequency of the homozygous mutant genotype, comparisons between the wild-type (C/C) and heterozygous (C/T) groups were performed using independent two-sample *t*-tests. SUA levels among the combined ABCG2 functional groups were compared using the Kruskal–Wallis test, followed by pairwise comparisons using the Mann–Whitney U test. Unadjusted odds ratios (ORs) and 95% confidence intervals (CIs) for hyperuricemia were calculated from contingency tables using the full-function ABCG2 group as the reference. Multivariable logistic regression was subsequently performed to estimate ORs adjusted for sex and age. Estimated ABCG2 function was included as a categorical variable with four levels (full, 3/4, 1/2, and ≤1/4), sex was included as a categorical covariate, and age was included as a continuous covariate. All 1653 participants were included in the analysis. Adjusted ORs, 95% CIs, and two-sided *p*-values were calculated using Wald statistics. A p-value < 0.05 was considered statistically significant. Cohen's κ coefficient was calculated to assess agreement between the real-time PCR assay and Sanger sequencing.

3. Results

3.1. Analytical Specificity of the Multiplex Real-Time PCR Assay for ABCG2 Genotyping

Analytical specificity was evaluated using four synthetic DNA templates individually representing the c.376C, c.376T, c.421C, and c.421A alleles of the *ABCG2* Q126X and Q141K variants. As shown in Figure 1, each allele-specific probe produced fluorescence only in the presence of its corresponding target allele, and no signal with the non-matching allele. The probe targeting the Q126X variant (c.376T) generated amplification exclusively with the c.376T template and not with the wild-type (c.376C) template (Figure 1B), whereas the probe targeting Q141K (c.421A) amplified exclusively the c.421A template (Figure 1D). No cross-reactivity or nonspecific amplification was observed for any of the probes. These results demonstrated high analytical specificity of the multiplex real-time PCR assay for discrimination of both *ABCG2* variants.

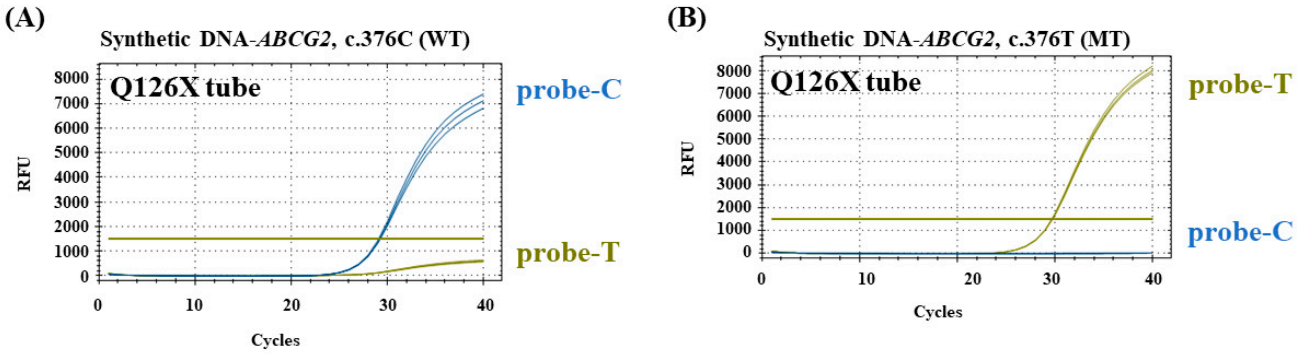


Figure 1. *Cont.*

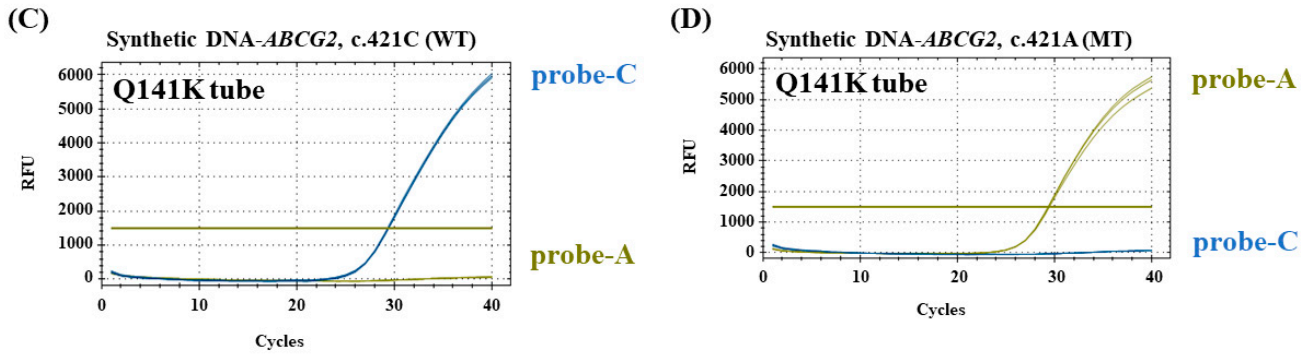


Figure 1. Analytical specificity assessment using synthetic DNA. Four synthetic DNAs corresponding to the *ABCG2* containing Q126X or Q141K variants [(**A**) *ABCG2*, c.376C (**B**) *ABCG2*, c.376T (**C**) *ABCG2*, c.421C (**D**) *ABCG2*, c.421A] were used to evaluate the assay's specificity. *ABCG2* synthetic DNA was selectively amplified using its respective probes, and no nonspecific amplification was observed. RFU, relative fluorescence unit. WT, wild-type. MT, mutant-type.

3.2. Assessment of Analytical Sensitivity

Analytical sensitivity was assessed using clinical DNA samples representing the four target alleles (c.376C, c.376T, c.421C, and c.421A), and the Ct values were summarized as mean ± SD (Table 2). Both c.376C and c.376T samples showed mean Ct values of 36.86 and 37.88, respectively, as low as 1×10^{-1} ng/µL, and the IC at 37.85 down to 1×10^{-2} ng/µL. Similarly, both c.421C and c.421A samples showed mean Ct values of 35.43 and 37.06, respectively, as low as 1 ng/µL, and the IC at 32.5 down to 1 ng/µL. In the clinical DNA dilution assessment, the lowest detected concentrations among the tested dilution levels were 1×10^{-1} ng/µL for Q126X and 1 ng/µL for Q141K.

Table 2. Analytical sensitivity of the assay using clinical specimens.

Target SNP	Fluorescence (Genotype)	*ABCG2* SNP Genotyping mRT-PCR Ct Values (Mean ± SD)						Lowest Detected Conc.* (ng/µL)
		Undiluted DNA Stock *	1×10^{1} ng/µL	1×10^{0} ng/µL	1×10^{-1} ng/µL	1×10^{-2} ng/µL	1×10^{-3} ng/µL	
Q126X (c.376C > T)	FAM (c.376C)	26.65 ± 0.15	29.65 ± 0.05	33.35 ± 0.06	36.86 ± 0.15	-	-	1×10^{-1}
	VIC (c.376T)	26.86 ± 0.09	30.55 ± 0.03	34.23 ± 0.12	37.88 ± 0.15	-	-	1×10^{-1}
	Cy5.5 (IC, *HBB*)	24.65 ± 0.35	27.55 ± 0.93	31.13 ± 0.85	34.63 ± 0.83	37.85 ± 0.89	-	1×10^{-2}
Q141K (c.421C > A)	FAM (c.421C)	27.21 ± 0.09	30.92 ± 0.36	35.43 ± 1.15	-	-	-	1×10^{0}
	VIC (c.421A)	27.67 ± 0.05	31.96 ± 0.16	37.06 ± 0.99	-	-	-	1×10^{0}
	Cy5 (IC, *HBB*)	25.90 ± 0.16	28.95 ± 0.13	32.50 ± 0.22	-	-	-	1×10^{0}

* Undiluted DNA stocks ranged from (5–8) × 10^{1} ng/µL and were first diluted to 1×10^{1} ng/µL; subsequent dilutions were 10-fold, down to 1×10^{-3} ng/µL.

Additional testing using the four synthetic plasmid DNA materials showed detection of c.376C and c.376T at 1×10^{-2} pg/reaction, with mean Ct values of 36.38 and 36.45, respectively, and c.421C and c.421A at 1×10^{-1} pg/reaction, with mean Ct values of 33.39 and 33.41, respectively (Supplementary Table S2). These results supplement the clinical DNA findings, particularly for the low-frequency c.376T allele.

3.3. Evaluation of Assay Precision

Intra-assay repeatability and inter-assay reproducibility were evaluated using 47 clinical specimens (Table 3A,B). Across genotype groups and fluorescence channels, pooled Ct

SDs ranged from 0.01 to 0.44 for intra-assay measurements, with corresponding descriptive Ct CVs of 0.05–1.46%. For inter-assay measurements across three independent runs on the same CFX96 instrument, pooled Ct SDs ranged from 0.08 to 0.55, with corresponding descriptive Ct CVs of 0.30–1.86%.

Table 3. Intra-assay repeatability and inter-assay reproducibility of multiplex real-time PCR assays for *ABCG2* Q126X and Q141K genotyping using clinical specimens.

(**A**) **Q126X (c.376C > T)**								
Genotype	**Fluorescence (Target)**	**No. of Specimens (*n*)**	**Intra-Assay ***			**Inter-Assay †**		
			Mean Ct	**SD ‡**	**CV (%)**	**Mean Ct**	**SD ‡**	**CV (%)**
C/C	FAM (c.376C)	28	26.70	0.20	0.76	26.57	0.17	0.64
	Cy 5.5 (IC, *HBB*)		24.87	0.19	0.75	24.95	0.21	0.86
C/T	FAM (c.376C)	18	28.20	0.11	0.39	27.98	0.22	0.78
	VIC (c.376T)		28.33	0.13	0.46	28.57	0.28	0.98
	Cy 5.5 (IC, *HBB*)		24.96	0.17	0.68	25.03	0.18	0.71
T/T	VIC (c.376T)	1	26.71	0.01	0.05	26.87	0.18	0.65
	Cy 5.5 (IC, *HBB*)		24.60	0.15	0.60	24.63	0.14	0.57
(**B**) **Q141K (c.421C > A)**								
Genotype	**Fluorescence (Target)**	**No. of Specimens (*n*)**	**Intra-Assay ***			**Inter-Assay †**		
			Mean Ct	**SD ‡**	**CV (%)**	**Mean Ct**	**SD ‡**	**CV (%)**
C/C	FAM (c.421C)	20	27.38	0.31	1.12	26.98	0.35	1.30
	Cy 5 (IC, *HBB*)		26.12	0.10	0.37	26.23	0.12	0.46
C/A	FAM (c.421C)	18	30.01	0.44	1.46	29.41	0.55	1.86
	VIC (c.421A)		30.34	0.23	0.75	30.65	0.46	1.50
	Cy 5 (IC, *HBB*)		26.52	0.08	0.32	26.59	0.08	0.30
A/A	VIC (c.421A)	9	27.60	0.17	0.62	27.77	0.29	1.05
	Cy 5 (IC, *HBB*)		26.01	0.07	0.27	26.15	0.17	0.64

* Intra-assay repeatability was assessed using duplicate measurements of each specimen within the same run. † Inter-assay reproducibility was assessed using measurements of the same specimens across three independent runs on the same instrument. ‡ SD represents the pooled within-sample SD across replicate measurements; CV (%) = SD/Mean Ct × 100.

3.4. Concordance of ABCG2 Genotyping with Sanger Sequencing

A total of 1653 clinical samples were successfully genotyped by both the multiplex real-time PCR assay and Sanger sequencing for method comparison (Table 4A,B). All samples yielded valid genotype calls for both Q126X and Q141K, corresponding to a call rate of 100% and a no-call rate of 0% (0/1653) for each variant. Complete concordance (100%) was observed between the two methods (Cohen's $\kappa = 1.00$) for both *ABCG2* variants, Q126X and Q141K, with no discordant genotype calls identified. The concordance included all genotype categories, including homozygous wild-type, heterozygous, and homozygous variant genotypes. However, Q126X was represented by 46 C/T specimens and only one T/T specimen; therefore, clinical validation of the Q126X homozygous variant genotype was limited to a single specimen. These findings demonstrate that the multiplex real-time PCR assay provides genotyping performance equivalent to that of Sanger sequencing and supports the use of the multiplex real-time PCR assay as a reliable and rapid method for routine *ABCG2* Q126X and Q141K genotyping, while further validation of the Q126X T/T genotype is needed.

Table 4. Concordance of *ABCG2* genotypes determined by multiplex real-time PCR and Sanger sequencing.

(**A**) **Q126X** (**c.376C > T**)					
ABCG2, exon4, c.376		Sanger sequencing			
		C/C	C/T	T/T	Total
Real-time PCR	C/C	1606	0	0	1606
	C/T	0	46	0	46
	T/T	0	0	1	1
	Total	1606	46	1	1653
(**B**) **Q141K** (**c.421C > A**)					
ABCG2, exon5, c.421		Sanger sequencing			
		C/C	C/A	A/A	Total
Real-time PCR	C/C	845	0	0	845
	C/A	0	677	0	677
	A/A	0	0	131	131
	Total	845	677	131	1653

Overall concordance = 100.0%; Cohen's κ = 1.00 for both variants.

Representative amplification plots generated by the multiplex real-time PCR assay and the corresponding Sanger sequencing chromatograms for all six genotypes (Q126X: C/C, C/T, and T/T; Q141K: C/C, C/A, and A/A) are provided in the Supplementary Figure S1.

3.5. Association Between ABCG2 Genotype Combinations and Hyperuricemia Risk

To demonstrate the clinical relevance of the developed assay, we evaluated the association between *ABCG2* combined genotypes (Q126X/Q141K) and hyperuricemia risk (Table 5). Individuals were classified into four functional groups (full, 3/4, 1/2, and ≤1/4 function) according to the estimated ABCG2 transport function described previously [19]. Reduced ABCG2 function was more frequent in the hyperuricemia group than in the control group, whereas the full-function genotype was more common in the control group (51.7% vs. 38.9%). Mean serum uric acid levels increased across groups with greater impairment of estimated ABCG2 function, from 5.13 mg/dL in the full-function group to 5.33, 5.57, and 6.12 mg/dL in the 3/4-, 1/2-, and ≤1/4-function groups, respectively. Compared with the full-function group, the corresponding unadjusted odds ratios (ORs) for hyperuricemia were 1.56, 2.07, and 3.29. After adjustment for sex and age using multivariable logistic regression, these associations remained statistically significant, with adjusted ORs of 1.57 (95% CI, 1.19–2.07; $p = 0.0012$), 2.07 (95% CI, 1.37–3.12; $p = 0.0005$), and 3.34 (95% CI, 1.30–8.57; $p = 0.0121$), respectively. These findings support the association between reduced estimated ABCG2 function and hyperuricemia after accounting for sex and age, and suggest the potential utility of combined Q126X/Q141K genotyping using the developed assay for genetic risk assessment.

Table 5. Serum uric acid levels and hyperuricemia risk associated with *ABCG2* combined genotypes of Q126X and Q141K.

Estimated ABCG2 Function	Combined Genotype		Hyper-uricemia †	Control	SUA (mg/dL)	*p*-Value (SUA) ‡	Unadjusted OR (95% CI)	Adjusted OR (95% CI)	Adjusted OR *p*-Value
	Q126X	Q141K	Number (%)	Number (%)					
≤1/4 Function	TT	CC	7 (2.4)	13 (1.0)	6.12± 2.32	0.1457	3.29 (1.28–8.41)	3.34 (1.30–8.57)	**0.0121**
	CT	CA							
1/2 function	CT	CC	40 (13.5)	118 (8.7)	5.57± 1.76	**0.0069**	2.07 (1.37–3.12)	2.07 (1.37–3.12)	**0.0005**
	CC	AA							
3/4 function	CC	CA	134 (45.3)	524 (38.6)	5.33± 1.49	**0.0267**	1.56 (1.19–2.05)	1.57 (1.19–2.07)	**0.0012**
Full function	CC	CC	115 (38.9)	702 (51.7)	5.13± 1.31	Reference	1.00 (Reference)	1.00 (Reference)	-

SUA levels are presented as mean ± SD. ORs and 95% CIs were calculated by contingency table analysis using the wild-type genotype combination as the reference. † Definition of hyperuricemia was serum uric acid levels of >7.0 mg/dL in men and >5.7 mg/dL in women. ‡ *p*-values were obtained by pairwise Mann–Whitney U tests comparing each functional group with the full-function group after a significant Kruskal–Wallis test. *p*-values < 0.05 are shown in bold. Adjusted ORs were estimated using multivariable logistic regression including estimated ABCG2 function, sex, and age as a continuous variable, with the full-function group as the reference. Adjusted OR *p*-values and 95% CIs were calculated using Wald statistics.

4. Discussion

Functional classification based on the combined *ABCG2* Q126X and Q141K genotypes has been established as a biologically meaningful framework for evaluating genetic susceptibility to hyperuricemia and gout. Matsuo et al. demonstrated that the combined effects of these two functional variants could be translated into estimated ABCG2 transport activity (full, 3/4, 1/2, and ≤1/4 function), with progressively reduced transporter function associated with increasing serum uric acid levels and gout risk [19]. Subsequent studies consistently reproduced these findings in East Asian populations and further demonstrated that this functional classification correlates not only with SUA concentrations and hyperuricemia but also with gout susceptibility and clinical outcomes, including mortality among patients receiving hemodialysis [32,43,44]. Rather than evaluating each SNP independently, the combined functional classification provides a biologically interpretable estimate of overall ABCG2-mediated urate transport capacity. Consistent with these previous reports, our study demonstrated that decreasing estimated ABCG2 function was associated with progressively higher SUA concentrations and increased odds ratios for hyperuricemia. These findings further support the clinical relevance of Q126X/Q141K genotyping for assessing inherited susceptibility to impaired urate excretion.

Although ABCG2 contributes to urate elimination, SUA concentrations also depend on uric acid production through purine catabolism. Purine degradation involves both deamination and oxidation: adenosine deaminase converts adenosine to inosine, guanine deaminase converts guanine to xanthine, and xanthine oxidoreductase catalyzes the successive oxidation of hypoxanthine to xanthine and xanthine to uric acid [45]. Dietary factors may influence these processes and gout risk. In a prospective study of men, higher meat and seafood intake was associated with greater gout risk, whereas higher dairy intake was associated with lower risk; purine-rich vegetable intake was not associated with increased risk [46]. Furthermore, a healthy lifestyle that included a healthy diet and no or moderate alcohol consumption was associated with lower gout risk across genetic risk categories [7,47]. Thus, urate homeostasis reflects the interplay between production and elimination, with both modifiable lifestyle factors and inherited variation in urate transport

contributing to susceptibility. In this context, combined *ABCG2* genotyping may complement SUA measurement by providing information on inherited susceptibility, although the benefit of genotype-guided dietary interventions was not evaluated in the present study.

To facilitate assessment of this inherited susceptibility, we developed a two-tube multiplex hydrolysis probe-based real-time PCR assay for genotyping the Q126X and Q141K variants. Unlike sequencing-based approaches designed for comprehensive variant discovery, the present assay specifically targets two predefined functional variants with well-established biological and clinical significance. This targeted strategy enables rapid and efficient genotyping while maintaining high analytical performance. The assay combines DPO primer technology with TaqMan MGB probes, thereby improving allele discrimination and minimizing nonspecific amplification during multiplex PCR. Analytical validation demonstrated high specificity without cross-reactivity, reliable genotype detection across clinically relevant DNA concentrations, and complete concordance with Sanger sequencing in 1653 clinical samples (Cohen's $\kappa = 1.00$). Together, these findings indicate that the assay provides sequencing-equivalent genotyping accuracy while offering a substantially simpler workflow and shorter turnaround time, making it well suited for routine molecular diagnostic laboratories.

Although several PCR-based methods for *ABCG2* genotyping have previously been described, relatively few studies have reported comprehensive analytical validation together with large-scale clinical validation using sequencing as the reference method. In the present study, analytical specificity, analytical sensitivity, and clinical concordance were systematically evaluated according to established molecular diagnostic validation principles. Complete agreement with Sanger sequencing across 1653 clinical specimens supports the analytical robustness of the assay and demonstrates its reliability for routine clinical genotyping. By enabling combined genotyping of the two functional *ABCG2* variants, Q126X and Q141K, the assay provides a practical approach for laboratories seeking standardized and high-throughput *ABCG2* genotyping. Such an assay may facilitate broader implementation of genetic testing for individuals with an inherited predisposition to hyperuricemia and may complement conventional biochemical assessment based on serum uric acid concentrations.

This study has several limitations. First, although Q126X is a functionally important variant, only one homozygous mutant sample was identified because of its low allele frequency in the study population, limiting clinical validation and genotype-specific analyses for this genotype. Further validation using additional T/T clinical specimens or well-characterized reference materials is needed. Second, the association analyses were based on serum uric acid-defined hyperuricemia rather than clinically confirmed gout. Although additional analyses adjusted for sex and age, other environmental and clinical factors influencing serum uric acid concentrations were not fully considered. Third, the primary assay validation was performed using genomic DNA extracted from EDTA whole blood, and comprehensive validation across other specimen types was not conducted. Further validation using a larger, genotype-diverse buccal swab cohort is required before routine implementation with this specimen type. Applicability to saliva, dried blood spots, alternative extraction methods, and defined long-term DNA storage and repeated freeze–thaw conditions remains to be established. Future studies involving larger and ethnically diverse populations, clinically characterized gout cohorts, and broader specimen-type validation will help establish the clinical utility of the assay and the generalizability of these findings.

In conclusion, we developed and analytically validated a multiplex real-time PCR assay for genotyping of the clinically relevant *ABCG2* Q126X and Q141K variants. The assay demonstrated robust analytical performance and complete concordance with Sanger sequencing, while accurately identifying genotype combinations associated with increased genetic susceptibility to hyperuricemia. This assay provides a practical molecular tool for

rapid *ABCG2* genotyping and may facilitate genetic risk assessment and routine laboratory implementation in populations at risk for hyperuricemia and gout.

Supplementary Materials: The following supporting information can be downloaded at: https://www.mdpi.com/article/10.3390/life16111800/s1, Supplementary Table S1: Serum uric acid levels according to *ABCG2* Q126X and Q141K genotypes, Supplementary Table S2: Analytical sensitivity assessment using synthetic DNA materials, Supplementary Figure S1: Representative amplification plots and Sanger sequencing chromatograms for six *ABCG2* genotypes.

Author Contributions: Conceptualization, M.Y.P. and Y.-J.Y.; methodology, K.-H.L. and H.S.J.; software, K.-H.L.; validation, K.-H.L., M.Y.P. and Y.-J.Y.; formal analysis, K.-H.L.; investigation, M.Y.P.; resources, D.M.; data curation, H.S.J.; writing—original draft preparation, K.-H.L. and M.Y.P.; writing—review and editing, D.M., Y.-H.S. and Y.-J.Y.; visualization, H.S.J. and Y.-H.S.; supervision, M.Y.P. and Y.-J.Y.; project administration, Y.-H.S. and Y.-J.Y. All authors have read and agreed to the published version of the manuscript.

Funding: This research received no external funding.

Institutional Review Board Statement: The study was conducted in accordance with the Declaration of Helsinki and approved by the Institutional Review Board of the Seegene Medical Foundation (SMF-IRB-2024-020 approved on 12 August 2024).

Informed Consent Statement: The requirement for patient consent was waived because leftover anonymized specimens were used for the study. The need for written consent from research participants was waived after approval from the competent Institutional Review Board that has authority over the presented cases. The legal compliance of this study was reviewed and approved by the Institutional Review Board of the Seegene Medical Foundation.

Data Availability Statement: The data that support the findings of this study are available from the corresponding author upon reasonable request.

Conflicts of Interest: The authors declare no conflicts of interest.

Abbreviations

The following abbreviations are used in this manuscript:

ANOVA	Analysis of variance
EDTA W/B	Ethylenediaminetetraacetic acid-anticoagulated whole blood
IC	Internal control
MAF	Minor allele frequency
MGB	Minor groove binding
PCR	Polymerase chain reaction
SUA	Serum uric acid

References

1. Zhu, Y.; Pandya, B.J.; Choi, H.K. Prevalence of gout and hyperuricemia in the US general population: The National Health and Nutrition Examination Survey 2007–2008. *Arthritis Rheum.* **2011**, *63*, 3136–3141. [CrossRef] [PubMed]
2. Taniguchi, A.; Kamatani, N. Control of renal uric acid excretion and gout. *Curr. Opin. Rheumatol.* **2008**, *20*, 192–197. [CrossRef] [PubMed]
3. Shi, X.; Zheng, F.; Wan, Q.; Chai, P.; Wang, G.; Pang, Z.; Ma, Y. Estimation of the current healthcare costs of gout in Liaoning Province from 2015 to 2022 based on the SHA2011 accounting system. *Front. Public Health* **2025**, *13*, 1646950. [CrossRef] [PubMed]
4. Fathallah-Shaykh, S.A.; Cramer, M.T. Uric acid and the kidney. *Pediatr. Nephrol.* **2014**, *29*, 999–1008. [CrossRef] [PubMed]
5. Du, L.; Zong, Y.; Li, H.; Wang, Q.; Xie, L.; Yang, B.; Pang, Y.; Zhang, C.; Zhong, Z.; Gao, J. Hyperuricemia and its related diseases: Mechanisms and advances in therapy. *Signal Transduct. Target Ther.* **2024**, *9*, 212. [CrossRef] [PubMed]
6. Sulem, P.; Gudbjartsson, D.F.; Walters, G.B.; Helgadottir, H.T.; Helgason, A.; Gudjonsson, S.A.; Zanon, C.; Besenbacher, S.; Bjornsdottir, G.; Magnusson, O.T.; et al. Identification of low-frequency variants associated with gout and serum uric acid levels. *Nat. Genet.* **2011**, *43*, 1127–1130. [CrossRef] [PubMed]

7. Zhang, Y.; Yang, R.; Dove, A.; Li, X.; Yang, H.; Li, S.; Wang, J.; Li, W.D.; Zhao, H.; Xu, W.; et al. Healthy lifestyle counteracts the risk effect of genetic factors on incident gout: A large population-based longitudinal study. *BMC Med*. **2022**, *20*, 138. [CrossRef] [PubMed]
8. Cho, S.K.; Kim, B.; Myung, W.; Chang, Y.; Ryu, S.; Kim, H.N.; Kim, H.L.; Kuo, P.H.; Winkler, C.A.; Won, H.H. Polygenic analysis of the effect of common and low-frequency genetic variants on serum uric acid levels in Korean individuals. *Sci*. *Rep*. **2020**, *10*, 9179. [CrossRef] [PubMed]
9. Dehghan, A.; Köttgen, A.; Yang, Q.; Hwang, S.J.; Kao, W.L.; Rivadeneira, F.; Boerwinkle, E.; Levy, D.; Hofman, A.; Astor, B.C.; et al. Association of three genetic loci with uric acid concentration and risk of gout: A genome-wide association study. *Lancet* **2008**, *372*, 1953–1961. [CrossRef] [PubMed]
10. Yang, B.; Mo, Z.; Wu, C.; Yang, H.; Yang, X.; He, Y.; Gui, L.; Zhou, L.; Guo, H.; Zhang, X.; et al. A genome-wide association study identifies common variants influencing serum uric acid concentrations in a Chinese population. *BMC Med*. *Genom*. **2014**, *7*, 10. [CrossRef] [PubMed]
11. Kolz, M.; Johnson, T.; Sanna, S.; Teumer, A.; Vitart, V.; Perola, M.; Mangino, M.; Albrecht, E.; Wallace, C.; Farrall, M.; et al. Meta-analysis of 28,141 individuals identifies common variants within five new loci that influence uric acid concentrations. *PLoS Genet*. **2009**, *5*, e1000504. [CrossRef] [PubMed]
12. Giri, A.K.; Banerjee, P.; Chakraborty, S.; Kauser, Y.; Undru, A.; Roy, S.; Parekatt, V.; Ghosh, S.; Tandon, N.; Bharadwaj, D. Genome wide association study of uric acid in Indian population and interaction of identified variants with Type 2 diabetes. *Sci*. *Rep*. **2016**, *6*, 21440. [CrossRef] [PubMed]
13. Tin, A.; Marten, J.; Halperin Kuhns, V.L.; Li, Y.; Wuttke, M.; Kirsten, H.; Sieber, K.B.; Qiu, C.; Gorski, M.; Yu, Z.; et al. Target genes, variants, tissues and transcriptional pathways influencing human serum urate levels. *Nat*. *Genet*. **2019**, *51*, 1459–1474. [CrossRef] [PubMed]
14. Köttgen, A.; Albrecht, E.; Teumer, A.; Vitart, V.; Krumsiek, J.; Hundertmark, C.; Pistis, G.; Ruggiero, D.; O'Seaghdha, C.M.; Haller, T.; et al. Genome-wide association analyses identify 18 new loci associated with serum urate concentrations. *Nat*. *Genet*. **2013**, *45*, 145–154. [CrossRef] [PubMed]
15. Matsuo, H.; Yamamoto, K.; Nakaoka, H.; Nakayama, A.; Sakiyama, M.; Chiba, T.; Takahashi, A.; Nakamura, T.; Nakashima, H.; Takada, Y.; et al. Genome-wide association study of clinically defined gout identifies multiple risk loci and its association with clinical subtypes. *Ann*. *Rheum*. *Dis*. **2016**, *75*, 652–659. [CrossRef] [PubMed]
16. Yamagishi, K.; Tanigawa, T.; Kitamura, A.; Köttgen, A.; Folsom, A.R.; Iso, H. The rs2231142 variant of the *ABCG2* gene is associated with uric acid levels and gout among Japanese people. *Rheumatology* **2010**, *49*, 1461–1465. [CrossRef] [PubMed]
17. Park, J.W.; Noh, J.H.; Kim, J.M.; Lee, H.Y.; Kim, K.A.; Park, J.Y. Gene Dose-Dependent and Additive Effects of ABCG2 rs2231142 and SLC2A9 rs3733591 Genetic Polymorphisms on Serum Uric Acid Levels. *Metabolites* **2022**, *12*, 1192. [CrossRef] [PubMed]
18. Nakayama, A.; Hayano, K.; Ueno, M.; Miyoshi, Y.; Nakashima, H.; Shimizu, S.; Hashimoto, I.; Toba, M.; Kikuchi, R.; Takehana, N.; et al. Dysfunctional variants of ABCG2 create strong individual and population risks for progression of hyperuricemia: The potential for implementation of genome-personalized nursing. *Hum*. *Cell* **2026**, *39*, 22. [CrossRef] [PubMed]
19. Matsuo, H.; Takada, T.; Ichida, K.; Nakamura, T.; Nakayama, A.; Ikebuchi, Y.; Ito, K.; Kusanagi, Y.; Chiba, T.; Tadokoro, S.; et al. Common defects of ABCG2, a high-capacity urate exporter, cause gout: A function-based genetic analysis in a Japanese population. *Sci*. *Transl*. *Med*. **2009**, *1*, 5ra11. [CrossRef] [PubMed]
20. Vitart, V.; Rudan, I.; Hayward, C.; Gray, N.K.; Floyd, J.; Palmer, C.N.; Knott, S.A.; Kolcic, I.; Polasek, O.; Graessler, J.; et al. SLC2A9 is a newly identified urate transporter influencing serum urate concentration, urate excretion and gout. *Nat*. *Genet*. **2008**, *40*, 437–442. [CrossRef] [PubMed]
21. Chen, C.J.; Tseng, C.C.; Yen, J.H.; Chang, J.G.; Chou, W.C.; Chu, H.W.; Chang, S.J.; Liao, W.T. ABCG2 contributes to the development of gout and hyperuricemia in a genome-wide association study. *Sci*. *Rep*. **2018**, *8*, 3137. [CrossRef] [PubMed]
22. Stark, K.; Reinhard, W.; Grassl, M.; Erdmann, J.; Schunkert, H.; Illig, T.; Hengstenberg, C. Common polymorphisms influencing serum uric acid levels contribute to susceptibility to gout, but not to coronary artery disease. *PLoS ONE* **2009**, *4*, e7729. [CrossRef] [PubMed]
23. Ohashi, Y.; Ooyama, H.; Makinoshima, H.; Takada, T.; Matsuo, H.; Ichida, K. Plasma and Urinary Metabolomic Analysis of Gout and Asymptomatic Hyperuricemia and Profiling of Potential Biomarkers: A Pilot Study. *Biomedicines* **2024**, *12*, 300. [CrossRef] [PubMed]
24. Hosomi, A.; Nakanishi, T.; Fujita, T.; Tamai, I. Extra-renal elimination of uric acid via intestinal efflux transporter BCRP/ABCG2. *PLoS ONE* **2012**, *7*, e30456. [CrossRef] [PubMed]
25. Asif, M.A.; Zulfiqar, Z.; Mustafa, B.E.; Nazir, U.; Sun, J.; Wang, Z.; Cui, Y.; Hao, S.; Liu, B.; Shi, Y. ABCG2 transporter: Structural and functional associations with gout (Review). *Int*. *J*. *Mol*. *Med*. **2026**, *58*, 235. [CrossRef] [PubMed]

26. Ichida, K.; Matsuo, H.; Takada, T.; Nakayama, A.; Murakami, K.; Shimizu, T.; Yamanashi, Y.; Kasuga, H.; Nakashima, H.; Nakamura, T.; et al. Decreased extra-renal urate excretion is a common cause of hyperuricemia. *Nat. Commun.* **2012**, *3*, 764. [CrossRef] [PubMed]
27. Zhang, L.; Spencer, K.L.; Voruganti, V.S.; Jorgensen, N.W.; Fornage, M.; Best, L.G.; Brown-Gentry, K.D.; Cole, S.A.; Crawford, D.C.; Deelman, E.; et al. Association of functional polymorphism rs2231142 (Q141K) in the ABCG2 gene with serum uric acid and gout in 4 US populations: The PAGE Study. *Am. J. Epidemiol.* **2013**, *177*, 923–932. [CrossRef] [PubMed]
28. Ye, J.; Zeng, Z.; Chen, Y.; Wu, Z.; Yang, Q.; Sun, T. Examining an Association of Single Nucleotide Polymorphisms with Hyperuricemia in Chinese Flight Attendants. *Pharmgenomics Pers. Med.* **2022**, *15*, 589–602. [CrossRef] [PubMed]
29. Liu, L.; Zhao, T.; Shan, L.; Cao, L.; Zhu, X.; Xue, Y. Estradiol regulates intestinal ABCG2 to promote urate excretion via the PI3K/Akt pathway. *Nutr. Metab.* **2021**, *18*, 63. [CrossRef] [PubMed]
30. Tu, H.P.; Ko, A.M.; Chiang, S.L.; Lee, S.S.; Lai, H.M.; Chung, C.M.; Huang, C.M.; Lee, C.H.; Kuo, T.M.; Hsieh, M.J.; et al. Joint effects of alcohol consumption and ABCG2 Q141K on chronic tophaceous gout risk. *J. Rheumatol.* **2014**, *41*, 749–758. [CrossRef] [PubMed]
31. Lukkunaprasit, T.; Rattanasiri, S.; Turongkaravee, S.; Suvannang, N.; Ingsathit, A.; Attia, J.; Thakkinstian, A. The association between genetic polymorphisms in ABCG2 and SLC2A9 and urate: An updated systematic review and meta-analysis. *BMC Med. Genet.* **2020**, *21*, 210. [CrossRef] [PubMed]
32. Nakashima, A.; Ichida, K.; Ohkido, I.; Yokoyama, K.; Matsuo, H.; Ohashi, Y.; Takada, T.; Nakayama, A.; Suzuki, H.; Shinomiya, N.; et al. Dysfunctional ABCG2 gene polymorphisms are associated with serum uric acid levels and all-cause mortality in hemodialysis patients. *Hum. Cell* **2020**, *33*, 559–568. [CrossRef] [PubMed]
33. Miyoshi, Y.; Nakayama, A.; Nakashima, H.; Hashimoto, I.; Kawamura, Y.; Shimizu, S.; Toyoda, Y.; Mizuno, T.; Tanabe, R.; Hamada, Y.; et al. Effects of ABCG2 dysfunction on hyperuricemia progression in premenopausal and postmenopausal women. *Hum. Cell* **2026**, *39*, 88. [CrossRef] [PubMed]
34. Matsuo, H.; Tsunoda, T.; Ooyama, K.; Sakiyama, M.; Sogo, T.; Takada, T.; Nakashima, A.; Nakayama, A.; Kawaguchi, M.; Higashino, T.; et al. Hyperuricemia in acute gastroenteritis is caused by decreased urate excretion via ABCG2. *Sci. Rep.* **2016**, *6*, 31003. [CrossRef] [PubMed]
35. Matsuo, H.; Ichida, K.; Takada, T.; Nakayama, A.; Nakashima, H.; Nakamura, T.; Kawamura, Y.; Takada, Y.; Yamamoto, K.; Inoue, H.; et al. Common dysfunctional variants in ABCG2 are a major cause of early-onset gout. *Sci. Rep.* **2013**, *3*, 2014. [CrossRef] [PubMed]
36. Woodward, O.M.; Köttgen, A.; Coresh, J.; Boerwinkle, E.; Guggino, W.B.; Köttgen, M. Identification of a urate transporter, ABCG2, with a common functional polymorphism causing gout. *Proc. Natl. Acad. Sci. USA* **2009**, *106*, 10338–10342. [CrossRef] [PubMed]
37. Rattanacheeworn, P.; Chamnanphon, M.; Thongthip, S.; Kittanamongkolchai, W.; Townamchai, N.; Avihingsanon, Y.; Udomnilobol, U.; Prueksaritanont, T.; Jianmongkol, S.; Chariyavilaskul, P. SLCO1B1 and ABCG2 Gene Polymorphisms in a Thai Population. *Pharmgenom. Pers. Med.* **2020**, *13*, 521–530. [CrossRef] [PubMed]
38. Matsuo, H.; Tomiyama, H.; Satake, W.; Chiba, T.; Onoue, H.; Kawamura, Y.; Nakayama, A.; Shimizu, S.; Sakiyama, M.; Funayama, M.; et al. ABCG2 variant has opposing effects on onset ages of Parkinson's disease and gout. *Ann. Clin. Transl. Neurol.* **2015**, *2*, 302–306. [CrossRef] [PubMed]
39. Chen-Xu, M.; Yokose, C.; Rai, S.K.; Pillinger, M.H.; Choi, H.K. Contemporary Prevalence of Gout and Hyperuricemia in the United States and Decadal Trends: The National Health and Nutrition Examination Survey, 2007–2016. *Arthritis Rheumatol.* **2019**, *71*, 991–999. [CrossRef] [PubMed]
40. Zhao, Q.; Wang, W.; Balati, A.; Zhang, B.; Li, C.; Guo, S.; Yu, D.; Chen, P. Association of hyperuricaemia and hyperglycaemia with risk of in-hospital mortality in acute aortic dissection: A multicentre cohort study in the Han Chinese population. *BMJ Open* **2025**, *15*, e094857. [CrossRef] [PubMed]
41. Kutyavin, I.V.; Afonina, I.A.; Mills, A.; Gorn, V.V.; Lukhtanov, E.A.; Belousov, E.S.; Singer, M.J.; Walburger, D.K.; Lokhov, S.G.; Gall, A.A.; et al. 3′-minor groove binder-DNA probes increase sequence specificity at PCR extension temperatures. *Nucleic Acids Res.* **2000**, *28*, 655–661. [CrossRef] [PubMed]
42. Chun, J.Y.; Kim, K.J.; Hwang, I.T.; Kim, Y.J.; Lee, D.H.; Lee, I.K.; Kim, J.K. Dual priming oligonucleotide system for the multiplex detection of respiratory viruses and SNP genotyping of CYP2C19 gene. *Nucleic Acids Res.* **2007**, *35*, e40. [CrossRef] [PubMed]
43. Zhou, D.; Liu, Y.; Zhang, X.; Gu, X.; Wang, H.; Luo, X.; Zhang, J.; Zou, H.; Guan, M. Functional polymorphisms of the ABCG2 gene are associated with gout disease in the Chinese Han male population. *Int. J. Mol. Sci.* **2014**, *15*, 9149–9159. [CrossRef] [PubMed]
44. Matsuo, H.; Nakayama, A.; Sakiyama, M.; Chiba, T.; Shimizu, S.; Kawamura, Y.; Nakashima, H.; Nakamura, T.; Takada, Y.; Oikawa, Y.; et al. ABCG2 dysfunction causes hyperuricemia due to both renal urate underexcretion and renal urate overload. *Sci. Rep.* **2014**, *4*, 3755. [CrossRef] [PubMed]
45. Kim, S.H.; Shin, J.; Son, H.E.; Kang, D.H. Role of urate transporters in the kidneys and intestine in uric acid homeostasis. *Kidney Res. Clin. Pract.* **2026**, *45*, 296–313. [CrossRef] [PubMed]

46. Choi, H.K.; Atkinson, K.; Karlson, E.W.; Willett, W.; Curhan, G. Purine-rich foods, dairy and protein intake, and the risk of gout in men. *N. Engl. J. Med.* **2004**, *350*, 1093–1103. [CrossRef] [PubMed]
47. Lai, Z.L.; Hung, Y.H.; Su, Y.D.; Lin, C.Y.; Li, Y.H.; Chen, C.Y.; Cho, D.Y.; Hsueh, P.R. Synergistic effects of ABCG2 Q141K variant in combination with alcohol consumption and male sex on gout risk in a rare-event Taiwanese cohort. *Sci. Rep.* **2026**, *16*, 9323. [CrossRef] [PubMed]

Disclaimer/Publisher's Note: The statements, opinions and data contained in all publications are solely those of the individual author(s) and contributor(s) and not of MDPI and/or the editor(s). MDPI and/or the editor(s) disclaim responsibility for any injury to people or property resulting from any ideas, methods, instructions or products referred to in the content.